Asian Journal of Pharmaceutical Sciences 15 (2020) 739–751

Available online at www.sciencedirect.com

ScienceDirect

journal homepage: www.elsevier.com/locate/AJPS

Original Research Paper

Regorafenib-loaded poly (lactide-co-glycolide) microspheres designed to improve transarterial chemoembolization therapy for hepatocellular carcinoma

Xiang Li[a,b], *Guangwei He*[c], *Feng Su*[c], *Zhaoxing Chu*[c], *Leiming Xu*[b], *Yazhong Zhang*[b], *Jianping Zhou*[a,*], *Yang Ding*[a,*]

[a] *State Key Laboratory of Natural Medicines, Department of Pharmaceutics, China Pharmaceutical University, Nanjing 210009, China*
[b] *Anhui Province Institute for Food and Drug Control, Hefei 230051, China*
[c] *Hefei Industrial Pharmaceutical Institute Co Ltd, Hefei 230051, China*

ARTICLE INFO

Article history:
Received 25 September 2019
Revised 28 December 2019
Accepted 18 January 2020
Available online 19 February 2020

Keywords:
Regorafenib
Microspheres
Transarterial chemoembolization
Hepatocellular carcinoma

ABSTRACT

Transarterial chemoembolization (TACE) has been widely introduced to treat hepatocellular carcinoma (HCC) especially for unresectable patients for decades. However, TACE evokes an angiogenic response due to the secretion of vascular endothelial growth factor (VEGF), resulting in the formation of new blood vessels and eventually tumor recurrence. Thus, we aimed to develop regorafenib (REGO)-loaded poly (lactide-co-glycolide) (PLGA) microspheres that enabled localized and sustained drug delivery to limit proangiogenic responses following TACE in HCC treatment. REGO-loaded PLGA microspheres were prepared using the emulsion-solvent evaporation/extraction method, in which DMF was selected as an organic phase co-solvent. Accordingly, we optimized the proportion of DMF, which the optimal ratio to DCM was 1:9 (v/v). After preparation, the microspheres provided high drug loading capacity of 28.6%, high loading efficiency of 91.5%, and the average particle size of 149 μm for TACE. IR spectra and XRD were applied to confirming sufficient REGO entrapment. The *in vitro* release profiles demonstrated sustained drug release of microspheres for more than 30 d To confirm the role of REGO-loaded microspheres in TACE, the cell cytotoxic activity on HepG2 cells and anti-angiogenic effects in HUVECs Tube-formation assay were studied in combination with miriplatin. Moreover, the microspheres indicated the potential of antagonizing miriplatin resistance of HepG2 cells *in vitro*. Pharmacokinetics preliminary studies exhibited that REGO could be sustainably released from microspheres for more than 30 d after TACE *in vivo*. *In vivo* anti-tumor efficacy was further determined in HepG2 xenograft tumor mouse model, demonstrating that REGO microspheres could improve the antitumor efficacy of miriplatin remarkably compared with miriplatin monotherapy. In conclusion,

* Corresponding authors. State Key Laboratory of Natural Medicines, Department of Pharmaceutics, China Pharmaceutical University, Nanjing 210009, China. Tel +86 25 83271102.
E-mail addresses: zhoujianp60@163.com (J.P. Zhou), dydszyzf@163.com (Y. Ding).
Peer review under responsibility of Shenyang Pharmaceutical University.

https://doi.org/10.1016/j.ajps.2020.01.001

the obtained REGO microspheres demonstrated promising therapeutic effects against HCC when combined with TACE.

1. Introduction

Transarterial chemoembolization (TACE) are broadly used against hepatocellular carcinoma (HCC) especially for inoperable patients for decades [1,2]. Conventional TACE usually involves intra-arterial administration of contrast medium and chemotherapeutic drugs via a catheter under image guidance, followed by embolization of the tumor-feeding artery with embolic agents (*e.g.*, gelatin sponge, degradable starch microspheres). For TACE with drug-eluting beads (DEB-TACE), chemotherapeutic drugs were encapsulated into the embolic microspheres prior to their transarterial delivery, which could execute dual-missions of occluding the selected vessels and controlling drug release. The embolic microspheres are usually classified into the non-biodegradable and biodegradable, which could both be applied for TACE [3,4].

The strategy of TACE can deliver high doses of chemotherapeutic drugs to tumors and also induce local ischemia and hypoxia via arterial embolization, which result in tumor necrosis and shrinkage. However, this ischemic or hypoxic variation of HCC after TACE induces the expression of vascular endothelial growth factor (VEGF) up-regulation and proangiogenic responses, leading to neoangiogenesis and eventually tumor recurrence [5–7]. Thus, TACE in combination with anti-angiogenic agents can decrease post-TACE angiogenesis and improve TACE therapy for HCC in theory. There have been a number of clinical trials conducted in this area. Most of them are combined regimens of oral antiangiogenic agents and TACE. These clinical trials results are inconclusive, some of them proved to be safe and promising [8–10]; while, the others were controversial and needed further research [11–13]. Compared to oral antiangiogenic agents, local delivery of microspheres loaded antiangiogenic agents together with TACE might offer a promising therapeutic regimen for HCC, with potentially enhanced therapeutic efficacy of TACE meanwhile reduced systemic exposures through drug entrapment in tumor-feeding vessels.

As an oral multikinase inhibitor, regorafenib (REGO) provides antiangiogenic activity in various tumor types by the inhibition of vascular endothelial growth factor receptors (VEGFR), tyrosine kinase with immunoglobulin and epidermal growth factor homology domain 2 (TIE-2), platelet-derived growth factor receptor-β (PDGFR-β), and fibroblast growth factor receptor (FGFR). The activity is correlated with suppression of cell proliferation, and induction of apoptosis by the inhibition of oncogenic kinases (KIT, RET, RAF-1, BRAF and mutant BRAF) [13,14]. It was approved for treating gastrointestinal stromal or metastatic colorectal cancer (mCRC) by the US Food and Drug Administration (FDA) [15,16]. In 2017, FDA approved REGO for a second-line therapy in previously sorafenib treated HCC patients [17]. Some commercial products of non-biodegradable microspheres have come into the market already such as DC Beads® and Hepasphere™ for TACE. Drugs especially the positively charged were usually shielded by ion exchange approach, and the drug elution kinetics were determined by the ionic environment of physiological fluids [4,18]. Compared with non-biodegradable microspheres, the biodegradable might expand the types of drug loading with adjustable drug release kinetics [19,20]. REGO is a hydrophobic drug that cannot be shielded into aforementioned microspheres (DC Bead®, Hepasphere™). In order to formulate REGO for TACE, we developed new biodegradable drug loading microspheres. These microspheres could better fine tune the flexible loading and release of the drug. As a biodegradable polymer approved by FDA, Poly(lactide-co-glycolide) (PLGA) has been widely applied in the preparation of various drug delivery platforms such as microspheres, implants, and *in situ* forming depots due to its biocompatibility and tunable properties [21,22]. The potential of PLGA microspheres prepared for TACE have been reported in several studies [23–25].

We aimed to develop REGO-loaded PLGA microspheres for improvement of TACE therapeutic effects, which can sustainably deliver REGO to limit proangiogenic responses in liver tumors after TACE. PLGA microspheres were prepared via the emulsion-solvent evaporation method with a cosolvent system. Physicochemical characterization of microspheres and the *in vitro* drug release were further investigated. Subsequently, the type and proportion of cosolvent were optimized. In order to confirm the role of REGO-loaded microspheres tailored to combine controlled local delivery and TACE, we introduced injectable miriplatin as chemotherapeutic drug used in TACE. Miriplatin is a highly lipophilic platinum derivative that can be delivered and suspended in Lipiodol for TACE in HCC treatment [26,27]. The *in vitro* biological activity in groups of blank microspheres, REGO microspheres, miriplatin, and REGO microspheres plus miriplatin has been further assessed for cytotoxicity and anti-angiogenic efficacy. *In vivo* pharmacokinetics of REGO microspheres and miriplatin were preliminarily evaluated in healthy adult New Zealand white male rabbits. The *in vivo* antitumor effects have also been investigated in HepG2 tumor models.

2. Materials and methods

2.1. Materials

PLGA (Mw: 34 000 Da; lactic acid/glycolic acid ratio 50:50) was purchased from Evonik Industries (Essen, Germany).

Polyvinyl alcohol (PVA, Mw: 30 000~70 000 Da) was from Guoren Yikang technology company (Beijing, China). Regorafenib and miriplatin for injection were kindly gifted from Hefei Industrial Pharmaceutical Institute Co. Ltd. (HeFei, China). MTT kit was bought from Sigma-Aldrich Co. (St Louis, USA). Matrigel® Matrix was from Corning Discovery Labware Inc. (Bedford, USA). RPMI 1640 medium, fetal bovine serum (FBS), penicillin streptomycin solution (pen-strep), endothelial cell culture medium (ECM), and endothelial cell growth supplement (ECGS) were purchased from Life Technologies Corporation (Grand Island, USA). Deionized water used in the experiments was prepared by a Millipore Milli-Q Water Purification System (Bedford, USA). Unless otherwise specified, all the chemicals were provided by Sinopharm Chemical Reagent Co. Ltd. (ShangHai, China).

2.2. Cell lines and culture conditions

Human hepatocarcinoma HepG2 cells were purchased from Procell Life Science Co. Ltd., (Wuhan, China). Miriplatin-resistant human hepatocarcinoma HepG2 cells (HepG2/MIRI) were established from their parental HepG2 cells by using pulse treatment with high concentration of miriplatin combining treatment with miriplatin of low concentration gradually increased and maintained in the presence of 0.2 μg/ml miriplatin. HepG2 cells and HepG2/MIRI Cells were cultured in RPMI 1640 medium supplemented with 10% FBS, 100 μg/ml streptomycin and 100 U/ml penicillin. Human umbilical vascular endothelial cells (HUVECs) from ScienCell Research Laboratories (Carlsbad, CA, USA) were maintained in ECM medium containing 5% (v/v) FBS and 1% (v/v) ECGS. All cells were incubated at standard cell culture condition (37 °C with 5% CO_2).

2.3. Animals

The BALB/c nude mice (20 ± 2 g) were purchased from the Shanghai Lingchang Biotechnology Co. Ltd (Shanghai, China). Adult New Zealand white male rabbits (2.0 ± 0.2 kg) were purchased from Nanjing Qinglongshan Animal breeding Co. Ltd (Nanjing, China). Animals were housed with a natural light–dark cycle, and acclimatized for 1 week prior to study. The rabbits were fasted 12 h before the study. The animal studies were approved by the China Pharmaceutical University Animal Ethics Committee.

2.4. Determination of REGO solubility

REGO solubility in dichloromethane (DCM), ethyl acetate (EA), acetone (AC), and dimethylformamide (DMF) were determined by incubating excess REGO in 1 ml of each solvent at 25 °C in a constant temperature air bath shaker at 100 rpm (rpm) for 24 h. REGO and solvent mixture were centrifuged for 10 min at the speed of 12 000 rpm to separate supernatant, then the supernatant were filtered using syringe filters (Clarinert™, Nylon, 0.22 μm). The filtered supernatant was diluted with the separated solvents and analyzed by Ultra Performance Liquid Chromatography (UPLC) using Waters ACQUITY H-Class (Milford, USA). Briefly, 1 μl of the supernatant was injected onto a Waters BEH C_{18} column (100 mm × 2.1 mm, 1.7 μm) with the column temperature of 35 °C.The mobile phase was acetonitrile-water (70:30, v/v) at the flow rate of 0.2 ml/min and the detection wavelength was 265 nm.

Table 1 – Preparation of REGO microspheres using various organic solvents. Data are expressed as the means ± SD ($n = 3$).

Solvents for preparation	Particle Size (μm)	LC (%)	LE (%)
DCM	98 ± 2.0	2.1 ± 0.1	83.6 ± 1.4
EA-DCM (1:9)	61 ± 1.0	3.7 ± 0.2	57.5 ± 2.1
AC-DCM (1:9)	56 ± 1.0	7.3 ± 0.5	48.4 ± 1.7
DMF-DCM (1:9)	149 ± 1.0	28.6 ± 0.3	91.5 ± 1.7

Table 2 – REGO microspheres preparation in various ratios of DMF-DCM. Data are expressed as the means ± SD ($n = 3$).

Solvent for preparation	Particle Size (μm)	LC (%)	LE (%)
DMF-DCM (1:9)	149 ± 1.0	28.6 ± 0.3	91.5 ± 1.7
DMF-DCM (1:4)	170 ± 2.0	27.9 ± 0.4	90.2 ± 1.5
DMF-DCM (3:7)	200 ± 1.0	29.6 ± 0.2	87.1 ± 0.9

2.5. Preparation of REGO microspheres

The controlled release microspheres of REGO were prepared by oil-in-water (O/W) emulsion-solvent evaporation method. PLGA (350 mg) and a specific amount of REGO (12–150 mg) were used in each of the formulation. PLGA and REGO were both dissolved in pre-designated 5 ml organic solvents (Table 1) followed by mixing using a vortex mixer. The solution was emulsified in 300 ml 1% PVA solution in a 1000 ml beaker by stirring at 500 rpm for 3 min with a magnetic stir bar. The stirring step was maintained at 200 rpm for 16 h to reach complete solvent evaporation. After 10 min and 1500 rpm centrifugation, the samples were further processed by vacuum filtration, washed with deionized water four times, and desiccated by freeze-lyophilized (overnight) to obtain the microspheres.

Moreover, REGO microspheres were prepared by varying the ratios of DMF and DCM. Briefly, PLGA (350 mg) and a specific amount of REGO (150 mg) were dissolved with the 5 ml mixture of DMF-DCM (Table 2). The preparation method of microspheres is the same as the method described above. The blank microspheres were prepared using the same method, except that REGO was not added.

2.6. Characterization of blank and REGO microspheres

Samples of REGO, blank microspheres, physical mixture of REGO with blank microspheres and REGO-loaded microspheres were analyzed via Infrared (IR) spectra (NICOLET iS10; Thermo Fisher, Massachusetts, USA). The samples were scanned in the range from 400 to 4000 cm^{-1}.

Additionally, X-ray powder diffraction (XRD) technique was applied to analyzing above four groups by X-ray diffractometer (SmartLab3; Rigaku, Tokyo, Japan). The samples were measured with the diffraction angle from 5° to 80°, 2θ angle.

2.7. Morphology and particle size

The surface morphology and shape of the microspheres was investigated through scanning electron microscopy (SEM) (Hitachi S-3700 N; Hitachi, Tokyo, Japan). Microsphere samples were mounted on the double-sided conductive adhesive attached to the sample plate and sputter-coated with gold. Particle size was measured with laser scattering device (Mastersizer 2000; Malvern instruments, Malvern, UK). The respective samples were suspended in water and subsequently, wet measurements of the microspheres size were performed. Particle size expressed as volume weighted mean diameter.

2.8. Drug loading evaluation

For drug loading assessment, 2 ml of DCM was added to 25 mg REGO microspheres, accurately weighed in 50 ml screw-cap tube, and soaked in a field of ultrasonic waves for 15 min with occasional shaking. Mobile phase (acetonitrile/water, 70:30, v/v) was added to dilute to volume followed by filtration using syringe filters (Clarinert^{TM}, Nylon, 0.22 μm). The amount of REGO encapsulated was evaluated by the UPLC method as described above. The drug loading capacity (LC) was calculated as loaded amount of REGO divided by the total microspheres weight. The loading efficiency (LE) was calculated as the loaded REGO divided by the total REGO amount feeding for encapsulation.

2.9. In vitro release studies

The automatic dissolution tester (SOTAX AT 7smart On-Line System; Sotax, Basel, Switzerland) were applied to evaluating controlled release behavior of REGO microspheres. It was studied using the paddle method with stirring speed at 100 rpm. The dissolution medium used was 800 ml pH 7.4 phosphate buffer containing 2% sodium dodecyl sulfate, maintained at 37.0 ± 0.5 °C. Approximately 10 mg of REGO microspheres were immersed in the dissolution medium, at predetermined time intervals (1 h, 4 h, 8 h, 12 h, 1 d, 2 d, 4 d, 6 d, 8 d, 10 d, 12 d, 16 d, 20 d, 25 d and 30 d), 5 ml samples were withdrawn and 5 ml fresh media was added. After filtering through syringe filters (Clarinert^{TM}, MCM, 0.22 μm), the REGO concentration in the filtrate were determined by the UPLC method as described above.

2.10. Effect of REGO on drug-resistance of HepG-2 induced by miriplatin

In the process of establishing drug-resistant cells HepG2/MIRI, HepG-2 cells were divided into four groups and induced by miriplatin in the presence of REGO at concentrations (0, 0.5, 1.0, 2.0 μmol/l) showing no or low cytotoxicity on the HepG-2 cells. The resistant cell lines are named accordingly as HepG2/MIRI-REGO 0, HepG2/MIRI-REGO 0.5, HepG2/MIRI-REGO 1.0 and HepG2/MIRI-REGO 2.0.

The resistant cell lines above-mentioned and HepG-2 cells with a density of 5×10^3 cells/well were inoculated into 96-well microplates. After treatment with miriplatin as designed, the IC_{50} of each cell line was determined by MTT method. After adding 20 μl MTT solution (5 mg/ml) to each well, and the plate was incubated for 4 h at 37 °C. The supernatants were removed and DMSO were added to dissolve the formazan product. Cell viability was analyzed by microplate reader (Power Wave TM XS; BIOTEX, northern Vermont, USA) at 570 nm. Cell viability (%) was calculated as (OD of test group/OD of control group) × 100%. To study the effect of REGO on drug resistance of HepG-2 induced by miriplatin, the IC_{50} values of miriplatin towards the resistant cell lines and HepG-2 cells were determined. The resistance index was calculated as the IC_{50} of the resistant cell lines divided by the IC_{50} of HepG-2 cells.

2.11. In vitro cytotoxicity studies

In vitro cytotoxicity of groups of blank microspheres, REGO microspheres, miriplatin, and REGO microspheres plus miriplatin against HepG2 cells were assessed by MTT assay. The four groups of samples were incubated in cell culture medium for 1 d, 3 d and 7 d at 37 °C, respectively, after which supernatants were collected. The HepG2 cells with a density of 5×10^3 cells/well were inoculated into 96-well microplates and treated with the supernatants for 48 h. The cytotoxicity of cells to samples was measured as previously described MTT method.

2.12. In vitro HUVECs tube-formation assay

The effect of released REGO on angiogenesis was evaluated by HUVECs Tube-formation Assay. After thawed on ice for 24 h, diluted matrigel was added into 96-well plates 50 μl per well then placed plates on ice bags for 10 min, cultured for 1 h at 37 °C to allow solidify. 2×10^4 HUVECs in ECM supplemented with 2% (v/v) FBS, 1% (v/v) ECGS (50 μl/well) were seeded into 96-well plates, an equal volume of supernatant (supernatant from microspheres of 7 d identical as for section "2.11") or bevacizumab (VEGF inhibitor, positive control) were also added into 96-well plates. After 10 h incubation, five areas were randomly selected for each group to photograph with an inverted microscope (DMi 8; Leica, Wetzlar, Germany) at 100-times magnification. The numbers of endothelial tubes in five different regions were analyzed with ImageJ software (Version 1.48v) and Angiogenesis Analyzer plug-in for ImageJ and its average value was applied to calculate tubule formation rate.

2.13. In vivo pharmacokinetics studies

Adult New Zealand white male rabbits weighing1.9–2.3 kg were introduced here. Under the X-ray digital subtraction angiography (X-ray DSA) (UNIQ FD10; Philips, Amsterdan, Netherlands) imaging, the rabbits received hepatic artery catheterization via femoral artery. After the success of catheter placement, miriplatin (15 mg/kg) plus REGO

microspheres (50 mg/kg) with 2 ml Iodized oil were infused, and then the catheter was withdrawn. At predetermined time intervals (1 h, 4 h, 8 h, 12 h, 1 d, 2 d, 4 d, 6 d, 8 d, 10 d, 12 d, 16 d, 20 d, 25 d and 30 d), 0.5 ml blood samples were collected from rabbit auricular vein. All the blood samples were centrifuged to extract the plasma and stored at −80 °C until analysis.

REGO concentrations were measured by LC/MS (ACQUITY UPLC-Xevo TQ-S; Waters, Milford, MA, USA). 50 µl acetonitrile containing 135 ng/ml sorafenib (internal standard) was pipetted into a polypropylene tube that contained 100 µl of plasma, and 850 µl of acetonitrile were added. After 3 min vortexing followed by 5 min centrifugation at 12 000 rpm, the supernatant was analyzed by using UPLC/MS system on a Waters BEH C_{18} column (100 mm × 2.1 mm, 1.7 µm) with the column temperature of 35 °C. The isocratic mobile phases consisted of 0.02% (v/v) formic acid in water–methanol (22:78, v/v) at the flow rate of 0.2 ml/min. The chromatographic run time was 6 min.

Miriplatin concentrations were measured by platinum (Pt) analysis using ICP-MS (X series 2; Thermo Scientific, Waltham, MA, USA) in standard instrument operation mode. The commentated tune solution was used to optimize the instrument parameter. The major isotope of platinum (Pt) was determined at *m/z* of 195, meanwhile, internal standard element indium (In) was determined at *m/z* 115. An aliquot of 0.2 ml rabbit plasma was added into a perfluoralkoxy (PFA) vessel (25 ml), adding 1.5 ml of HNO_3 (65%) and 0.5 ml of HCl (37%). Then the microwave-assisted acid digestion was performed using a microwave (MARS 6, CEM, Matthews, NC, USA). Prior to ICP-MS analysis, the sample solutions were diluted to 10 ml with deionized water. The pharmacokinetic parameters were calculated from the average REGO and miriplatin (Pt) concentrations in the bloodstream using Kinetic 4.4.1.

2.14. *In vivo evaluation in a HepG2 xenograft tumor model*

A HepG2 xenograft tumor model was established in female BALB/c nude mice, which was applied to determine the *in vivo* anti-tumor activity of REGO microspheres and/or miriplatin. Female BALB/c mice (4–5 weeks old) were implanted at the right armpit by subcutaneous injection with HepG2 tumor cells (3×10^6/0.2 ml PBS). When tumor size was approx. 150–200 mm^3, 24 BALB/c mice were randomized into 4 groups of 6 animals each. Subsequently, animals in four groups were treated with blank microspheres (control, 200 mg/kg), REGO microspheres (200 mg/kg), miriplatin alone (25 mg/kg) and REGO microspheres (200 mg/kg) plus miriplatin (25 mg/kg), respectively. In four groups, mice were treated by intratumorally injection with samples suspended in 100 µl Iodized oil, which were used immediately after preparation. Animal weights were recorded during the experiments. Tumor length (L), width (W) were measured and tumor volume (TV) was calculated as $TV=1/2 \times L \times W^2$. After 17 d of observation, animals were sacrificed, and then the tumor tissues were excised and weighed. Tumor growth inhibition was defined as the ratio of mean tumor volume of treated group compared with control group at the time of sacrifice of the mice.

2.15. *Data analysis*

The data analysis of different groups was conducted with one-way ANOVA in GraphPad Prism 5 software. The significant level were considered at $P < 0.05$ and greatly significant at $P < 0.001$. All data are presented as mean ± SD. (Unless otherwise stated, $n = 3$)

3. Results and discussion

3.1. *Determination of REGO solubility in organic solvents*

Clinically, non-biodegradable microspheres (*e.g.* DC Beads® and Hepasphere™) have been widely used in TACE for HCC treatment. However, since poor water solubility, REGO cannot be readily loaded into the microspheres by ion exchange. To deliver the hydrophobic drug, REGO microspheres were developed via the oil in water (O/W) emulsion-solvent evaporation, a commonly used method for microencapsulating of hydrophobic drugs. Herein, PLGA was introduced for microsphere fabrication, firstly which dissolved along with drug in the organic phase. Thus, it is essential to determine REGO solubility in various solvents (*e.g.* DCM, EA, AC and DMF) potentially applicable for microsphere preparation. We measured REGO solubility of these solvents, and found that the values of REGO solubility was 2.71 ± 0.06, 15.16 ± 0.17, 32.63 ± 0.26, and 410.34 ± 2.65 mg/ml in DCM, EA, AC and DMF at 25 °C, respectively. According to the description of solubility in the United States Pharmacopoeia (USP), REGO is only slightly soluble in DCM (one of the most desirable solvents in O/W emulsion method), sparingly soluble in EA and AC, but freely soluble in DMF. Due to low solubility of REGO in DCM, EA and AC, and undesirable for microsphere preparation (water-miscible DMF), single solvent is not suitable for preparing REGO/PLGA microspheres. Alternatively, a cosolvent system may be added to DCM for preparation of REGO/PLGA microspheres; and as reported, solvents of EA, AC and DMF have been proposed as cosolvent [28–30].

3.2. *Preparation of REGO microspheres using various organic solvents*

As described above, single solvent is not appropriate for fabricating the microspheres. For example, the LC of REGO/PLGA microspheres prepared using DCM alone was only 2.1%. For the development of REGO microspheres with high loading efficiency, we tested EA, AC and DMF as cosolvent with DCM. As results shown in Table 1, when EC, AC and DMF were used as cosolvent with DCM, the LC of microspheres increased to 3.7%, 7.3% and 28.6%, respectively.

The LE of the microspheres prepared by EA and AC as cosolvent of DCM was 57.5% and 48.4%, respectively, which was significantly lower than that of the microspheres prepared by DCM single solvent (83.6%). In comparison, LE for that of the microspheres obtained from DMF as cosolvent with DCM was 91.5%. As the capacity for dissolution of polymer and drug, the characteristics including interfacial tension of solvent, solubility of solvent in water and viscosity,

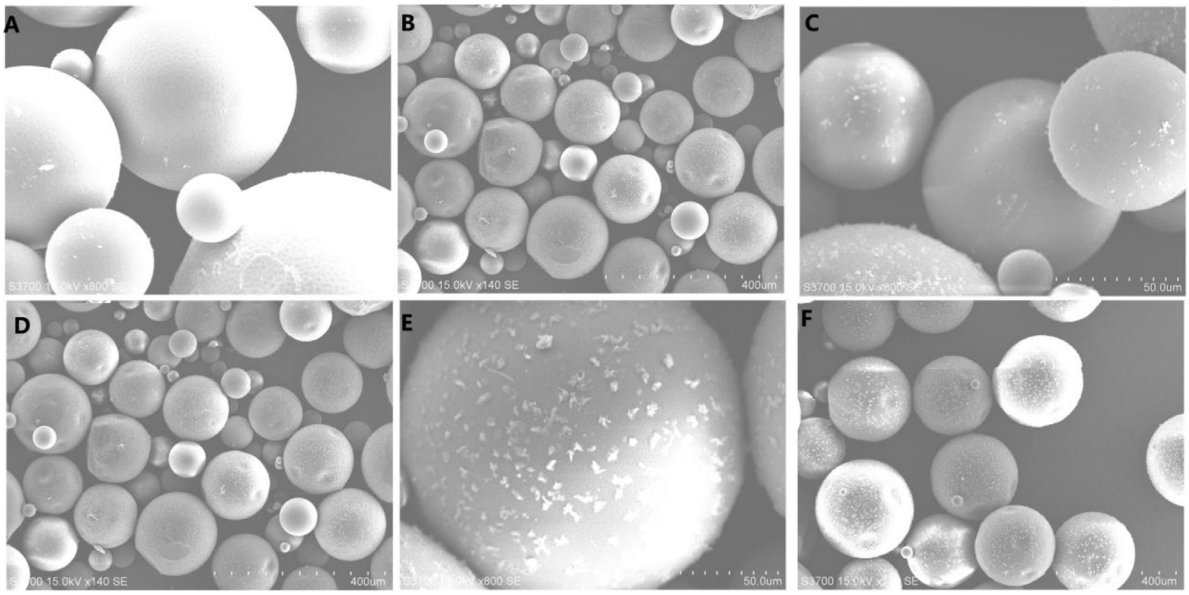

Fig. 1 – SEM images of REGO microspheres in various ratios of DMF-DCM. (A) and (B) for DMF-DCM (1:9); (C) and (D) for DMF-DCM (1:4); (E) and (F) for DMF-DCM (3:7). (A) (C) (E) is 800×; (B) (D) (F) is 140×.

need to be further considered (**Appendix**) [51–53], since they usually affect the LE and particle size of the microspheres. In this study, the insolubility in water and higher solubility in organic phase of REGO were beneficial to improving LE of microspheres. We also found that the high interfacial tension of organic solvent is desirable in terms of improving the LE of microspheres; meanwhile, with the increase of the interfacial tension, the particle size of microspheres increased correspondingly, similar to previous reports [31,32]. In addition, the solubility of solvent in water may also influence LE of microspheres [33]. Last but not the least, the LE difference of microspheres obtained from AC and DMF might be due to not only the balance between the two factors mentioned above, but also the viscosity of the polymer solution. The higher viscosity (0.802 cP) of DMF compared to that (0.316 cP) of AC might also contribute to the enhancement of LE in microspheres.

The optimal microspheres formulation should possess reasonably high LC and LE. For instance, multiple hydrophobic drug-loaded polymeric microspheres have been reported for TACE treatment with cisplatin LC of 2.4% for poly (D,L-lactic acid) microspheres in DCM [20], sorafenib LC of 15.7% for poly (D,L-lactic acid) microspheres in dimethyl sulphoxide plus DCM [20], and sorafenib LC of 18.6% for PLGA microspheres in dimethyl sulphoxide plus DCM [24]. In contrast to the previous studies, the obtained REGO microspheres could achieve high LC (28.6%) and LE (91.5%) by using the desired DMF-DCM cosolvent system. It was a common opinion that microspheres with diameters ranging from 40 to 1000 μm would be desirable [34]. The average particle size of 149 μm for the prepared microspheres was suitable for TACE. From the results described above, it is observed that DMF as cosolvent with DCM gave appropriate characterizations of LC, LE and particle size in microsphere formulation. It is worth to mention that PLGA microspheres via using cosolvent system could also be applied as platforms to deliver poorly water soluble, potent but costly drugs (e.g., sorafenib, cisplatin and paclitaxel).

3.3. *REGO microspheres preparation in various ratios of DMF-DCM*

3.3.1. *REGO microspheres preparation in various ratios of DMF-DCM*

Collectively, the preparation of REGO microspheres via using DMF-DCM is the optimal cosolvent system. The difficulty still remained whether the ratios of DMF and DCM would affect the performance of REGO microspheres including LC, LE, particle size, surface morphology and release profiles *in vitro*. Accordingly, the ratios of DMF and DCM were selected at 1:9, 1:4 or 3:7 to prepare REGO microspheres, and the effects of ratios of DMF and DCM on microspheres were further examined. As shown in Table 2, the particle size of microspheres was 149, 170 and 200 μm, respectively, increased with the augment of the DMF proportion. As discussed above, the augment of DMF proportion might increase interfacial tension of mixed solvents, accordingly cause the increase of particle size of the microspheres. The LC and LE of the microspheres were 27.9%–29.6% and 87.1%–91.5%, without significant differences while changing the proportion of DMF.

3.3.2. *Morphology of REGO microspheres in various ratios of DMF-DCM*

By the observation of SEM, surface morphology of REGO microspheres in various ratios of DMF-DCM were shown in Fig. 1. With the increase of DMF proportion, there were more and more pits on the surface of microspheres. Meanwhile, the drug particles also increased accordingly on the surface of microspheres. It was speculated that during the microsphere preparation, DMF partitions into the aqueous phase resulted

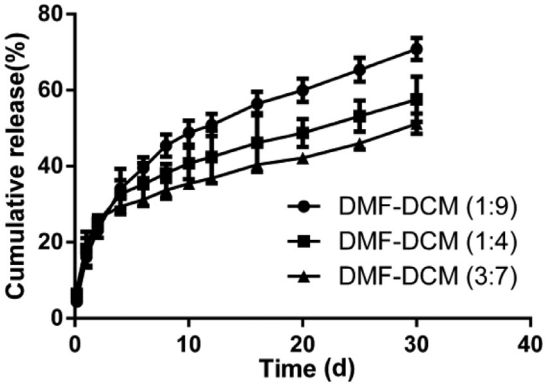

Fig. 2 – REGO release profiles from microspheres in various ratios of DMF-DCM. Data are expressed as the means ± SD ($n = 3$).

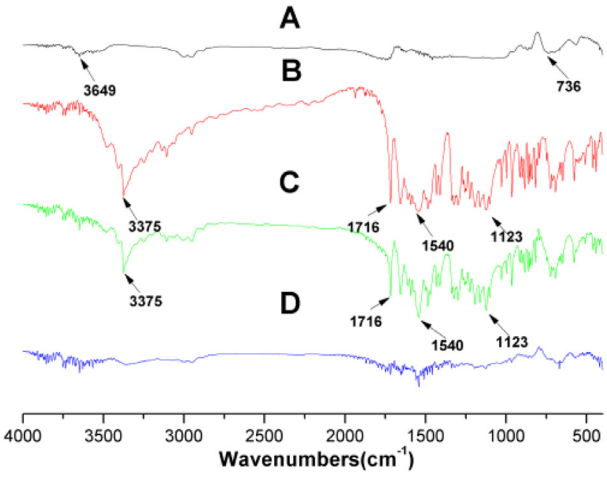

Fig. 3 – Infrared spectra of (A) blank microspheres, (B) REGO, (C) physical mixture of blank microspheres and REGO and (D) REGO microspheres.

in REGO precipitation at the polymer-water interface, owing to the poor aqueous solubility of REGO.

3.3.3. *In vitro release of REGO microspheres in various ratios of DMF-DCM*

The solubility of regorafenib in dissolution medium at 37 °C was 26.28 μg/ml, which was measured reference to the method described in Section 2.4. The release profiles of REGO from the microspheres were illustrated in Fig. 2. Even though the microspheres of different formulations gave similar LC, it appears that they displayed different release profiles *in vitro*. Overall, all formulations exhibited biphasic release pattern during 30-d period: first phase was an initial burst release; secondary phase was a more sustained release. In the first 2 d release intervals, the microspheres prepared in ratios of 1:9, 1:4, 3:7 for DMF and DCM initially released about 23.1%, 25.2% and 26.1%, respectively. The initial burst release could be due to the drug diffused from the particles on the surface of microspheres. And in our case, REGO microspheres surface may contain high amount of drug particles due to higher drug-loading, which might promote the occurrence of burst release [35]. Recent studies have demonstrated that patient serum/plasma VEGF levels increased significantly within the first 24 h after TACE, suggesting an undesirable neoangiogenetic reaction [36,37]. As we developed REGO-loaded PLGA microspheres to limit proangiogenic responses for TACE, the initial burst of REGO might be beneficial for clinical application to synchronize with and act on the first 24 h rising of VEGF levels. At 30 d, the release percentage of REGO from the microspheres prepared in ratios of 1:9, 1:4, 3:7 for DMF and DCM were 70.8%, 57.6% and 51.2%, respectively. The 30-day release decreased with the increase of DMF ratio, and the lower release of REGO might be explained by the increase of particle size of the microspheres. The different release behaviors of the obtained microspheres were affected by their physicochemical properties such as morphology, particle size and drug loading. Like process parameters, multiple competing factors such as solubility of drug in the organic phase, interfacial tension between solvent (cosolvent) and water, the viscosity of the polymer phase, and solubility of solvent in water could also affect the aforementioned physicochemical properties. This certainly increased the complexity of drug release, meanwhile provided numerous possible ways to fulfill the adjustable release [38,39]. The drug release profile would indeed offer more treatment options for TACE therapy. Collectively, the microspheres provided a platform to better adjust the loading of the drug(s), particle size and the release pattern, which could meet the requirements of various drug delivery systems. The dissolution pattern of the formulation in ratios of 1:9 for DMF and DCM was optimal for the desired (highest) 30-d sustained release in our study. In the subsequent experiments, we chose the microspheres prepared in ratios of 1:9 for DMF and DCM for further investigation.

3.4. *Characterization of blank microspheres and REGO microspheres*

The morphology of REGO microspheres from SEM has confirmed the successful formation of REGO microspheres. For further verification, we utilized Infrared spectra and X-ray powder diffraction to characterize the prepared microspheres. As shown in Fig. 3 of IR spectra, REGO shared characteristic absorption peaks at 1123, 1540, 1716 and 3375 cm^{-1}. These absorption peaks still existed in the physical mixture of blank microspheres with REGO except for the intensity decreased. As REGO microspheres, these absorption peaks almost disappeared.

As XRD profiles shown in Fig. 4, REGO gave crystal diffraction peaks in the range of 10°–35°, indicating that REGO existed in the form of crystal. Similar to IR spectra, these characteristic peaks still presented in the physical mixture of blank microspheres and REGO; however, the intensity decreased simultaneously. It was observed that the characteristic peaks for REGO in XRD pattern could not be found in REGO microspheres. The results of IR and XRD images suggested that REGO were embedded in the skeleton of PLGA microspheres and did not exist in a mixed form.

Table 3 – IC_{50} values of miriplatin and the resistance index of cell lines. Data are expressed as the means ± SD ($n = 5$).

Cell lines	Induced drug	IC_{50} values (μg/ml)	Resistance index
HepG-2	/	2.21 ± 0.03	/
HepG2/MIRI-REGO 0	Miriplatin	30.08 ± 0.61***	13.61
HepG2/MIRI-REGO 0.5	Miriplatin + REGO (0.5 μmol/l)	14.43 ± 0.27***	6.53
HepG2/MIRI-REGO 1.0	Miriplatin + REGO (1.0 μmol/l)	12.80 ± 0.47***	5.79
HepG2/MIRI-REGO 2.0	Miriplatin + REGO (2.0 μmol/l)	6.43 ± 0.32***	2.91

*** $P < 0.001$, compared with HepG-2.

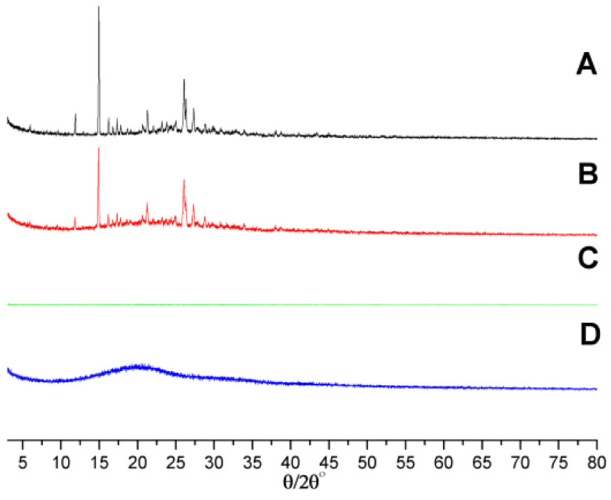

Fig. 4 – XRD profiles of (A) REGO, (B) physical mixture of blank microspheres and REGO, (C) REGO microspheres, and (D) blank microspheres.

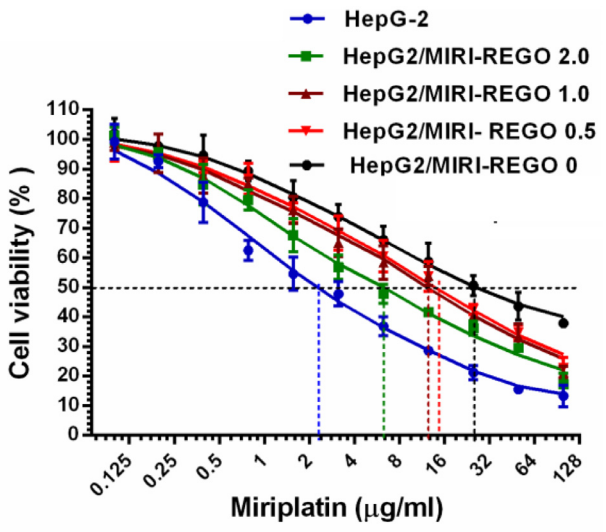

Fig. 5 – Effects of REGO on drug resistance of HepG-2 cells induced by miriplatin. Data are expressed as the means ± SD ($n = 5$).

3.5. *Effect of REGO on drug resistance of HepG-2 induced by miriplatin*

In our study, we introduced injectable miriplatin as chemotherapeutic drug for TACE. Considering that the cytotoxic chemotherapeutics are susceptible to drug resistance in the treatment of HCC, we introduced REGO for the remedy. In previous studies, REGO could antagonistic the resistance of paclitaxel associated with ABCB1 transporter on colorectal tumors in mice [40]. We determined the cytotoxicity of miriplatin on HepG-2 cells and the resistant cell lines, and the effect of REGO on the resistant cell lines induced by miriplatin was further evaluated. The IC_{50} values of miriplatin and the resistance index of resistant cell lines were summarized in Table 3. HepG2/MIRI-REGO 0 cell displayed resistance to miriplatin with IC_{50} of (30.08 ± 0.27) μg/ml, as well as the resistance index of 13.61 as compared to HepG-2 cells. Upon REGO action in the process of establishing drug-resistant cells, the sensitivity of the drug resistant cell HepG2/MIRI-REGO 0.5, HepG2/MIRI-REGO 1.0, HepG2/MIRI-REGO 2.0 to miriplatin was enhanced, and evidenced by greatly significant decrease in IC_{50} values ($P < 0.001$) of 14.43 ± 0.27, 12.80 ± 0.47 and 6.43 ± 0.32 μg/ml, respectively. Meanwhile, the resistance index was also decreasing as 6.53, 5.79 and 2.91, respectively.

As demonstrated in Fig. 5, the IC_{50} values were reduced with the increase of REGO concentration during induction, resulting in a leftward shift of the concentration-response curve. In the present study, REGO performed intensive effects on reversing drug resistance of HepG-2 cells *in vitro*. These results demonstrated the potentiation of the anticancer effects of miriplatin in drug resistant cells by REGO, suggesting the concept that REGO microspheres might perform the potential of antagonizing miriplatin resistance continuously when co-administered in clinical TACE.

3.6. *In vitro cytotoxicity studies*

The above results of REGO function on the resistant cell lines indicated that REGO could increase the sensitivity of HepG2 cells to miriplatin. The *in vitro* biological activity in groups of blank microspheres, REGO microspheres, miriplatin, and REGO microspheres plus miriplatin were further assessed for cytotoxicity. The viability of HepG2 cells with various preparations were shown in Fig. 6. Supernatants from blank microspheres were non-cytotoxic and adopted as control. It was found that supernatants from REGO microspheres and

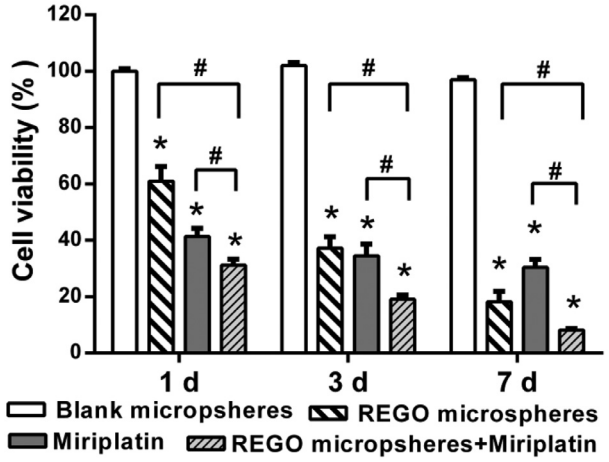

Fig. 6 – Cytotoxic effects of sample supernatants obtained for different incubation time (1 d, 3 d or 7 d) on HepG2 cell viability. Data are expressed as the means ± SD ($n = 5$). $^{*}P < 0.05$, compared with control, $^{\#}P < 0.05$ between conditions.

miriplatin alone or in combination significantly inhibited cell proliferation compared to the control group at the indicated time points (Fig. 6). Interestingly, it exhibited significant inhibition of the combinatorial group compared to the monotherapy for different incubated time (1 d, 3 d or 7 d). It is worth noting that with the increase of incubation time, the inhibitory effect of the combinatorial group was more remarkable. The cell viability of HepG2 in the combinatorial group for one day-incubation was 31.2% compared to the miriplatin monotherapy group of 41.4%, while that for 7 d-incubation was only 8.2% compared to the miriplatin monotherapy group of 30.4%.

The superior efficacy in combinatorial treatment group could inhibit or block the related factors of cell proliferation and survival with different mechanisms of action. Moreover, the outstanding functions of REGO might contribute to the decrease of the drug resistance of HepG2 cells induced by miriplatin. Accordingly, REGO could obtain the similar therapeutic outcomes in combination with other conventional chemotherapeutic agents. Synergistic antitumor effects were observed with the addition of REGO to 5-fluorouracil in multiple human colorectal cancer cell lines [41]. In another study, it was found that REGO potentiated antitumor effect of topotecan in the mitoxantrone-resistant xenograft model [42]. The results presented in Fig. 6 indicated that REGO microspheres could continuously enhance miriplatin cytotoxic activity *in vitro* and might be effectively applied in TACE together with miriplatin.

3.7. *In vitro HUVECs tube-formation assay*

From above *in vitro* cytotoxicity studies, REGO microspheres have demonstrated the inhibition of tumor cell proliferation. In order to evaluate the anti-angiogenesis effect of REGO microspheres, HUVECs tube formation assay was performed in different samples for 7 d incubation, in which VEGF inhibitor (bevacizumab) as positive control. As shown in Fig. 7A and 7B, supernatants from miriplatin or blank microspheres revealed no inhibitory effects on tube formation, with counting results of endothelial tubes comparable to untreated control. Supernatants of REGO microspheres and REGO microspheres plus miriplatin inhibited tube formation significantly, with comparable inhibitory levels to bevacizumab group. The results implied that REGO released from the microspheres resulted in anti-angiogenic effects, consistent with the expected results of REGO microspheres in our design. It could be found that REGO microspheres not only inhibited the tumor cells proliferation but also tumor neovascularization.

Table 4 – Plasma PK parameters of miriplatin (Pt) and REGO after TACE in rabbits. Data are expressed as the means ± SD ($n = 6$).

Parameters	Miriplatin (Pt)	REGO
$T_{1/2}$ (h)	607.9 ± 145.6	576.8 ± 68.8
T_{max} (h)	14.0 ± 4.9	68.0 ± 108.6
C_{max} (ng/ml)	395.2 ± 84.1	2.5 ± 0.4
AUC_{0-t} (h·ng/ml)	203,131.5 ± 56,881.4	950.6 ± 179.3
$AUC_{0-\infty}$ (h·ng/ml)	368,008.1 ± 101,657.9	1792.0 ± 447.2

3.8. *In vivo pharmacokinetics study*

To further confirm the sustained release of REGO from the microspheres *in vivo*, plasma levels of miriplatin (Pt) and REGO measured at predetermined time points after TACE were shown in Fig. 8. Plasma concentrations of miriplatin (Pt) decreased slowly; and the concentration was still at 192.8 ng/ml after 30 d, that was approximately half of C_{max} (395.2 ng/ml). Meanwhile, plasma concentrations of REGO decreased slowly, of which the concentration was maintained at 1.0 ng/ml until 30 d, approximately 2/5 of C_{max} (2.5 ng/ml). As listed in Table 4, the plasma elimination half-life ($T_{1/2}$) for miriplatin (Pt) and REGO was 607.9 h and 576.8 h, respectively. The results revealed that REGO could be released from microspheres sustainably for more than 30 d *in vivo*. This sustained release kinetics *in vivo* might potentiate therapeutic effects continuously after TACE as we proposed.

3.9. *In vivo antitumor efficacy in HepG2 xenograft tumor model*

Considering the promising *in vitro* biological activity and desirable PK profiles, the *in vivo* pharmacological efficacy was further investigated in a HepG2 xenograft tumor model. In the experimental process, body weight of animals in each group was stable. It suggested that the experimental doses in all groups were tolerable. As shown in Fig. 9A, we found an obvious retardation of tumor growth for animals treated with REGO microspheres, miriplatin alone, or in combination, as compared to the control group. Most importantly, treatment with the combination of REGO microspheres and miriplatin could significantly enhance the efficacy of chemotherapy for miriplatin alone, as evidenced by more remarkable slow-down for tumor growth in relative to the miriplatin

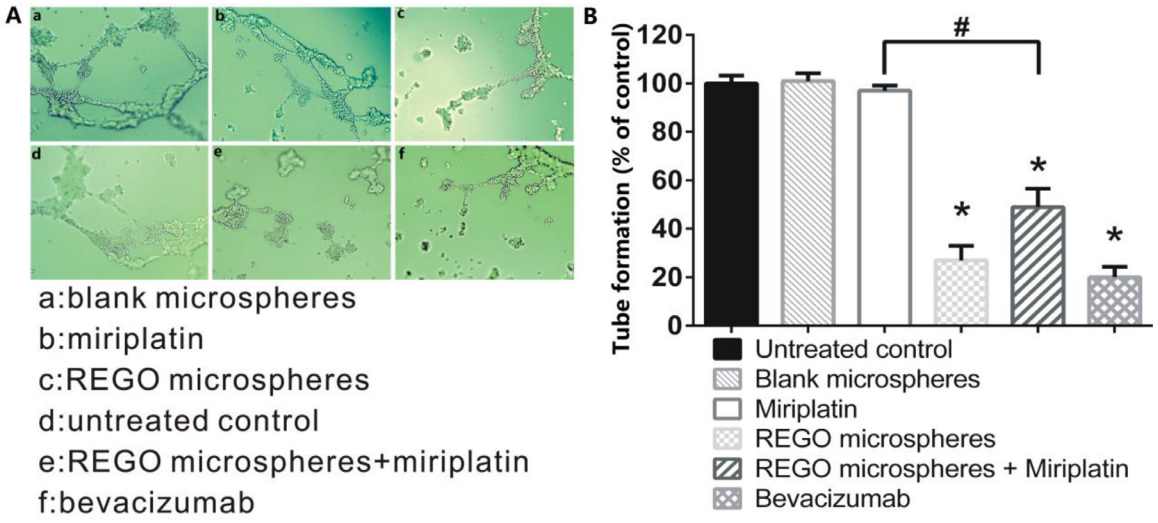

Fig. 7 – The effects of bevacizumab as VEGF inhibitor (positive control) and supernatants of samples on endothelial tube formation. (A) Representative photomicrographs of endothelial tube assay. (B) Counting results of endothelial tubes. Data are expressed as the means ± SD ($n = 5$). *$P < 0.05$, compared with untreated control, #$P < 0.05$ between conditions.

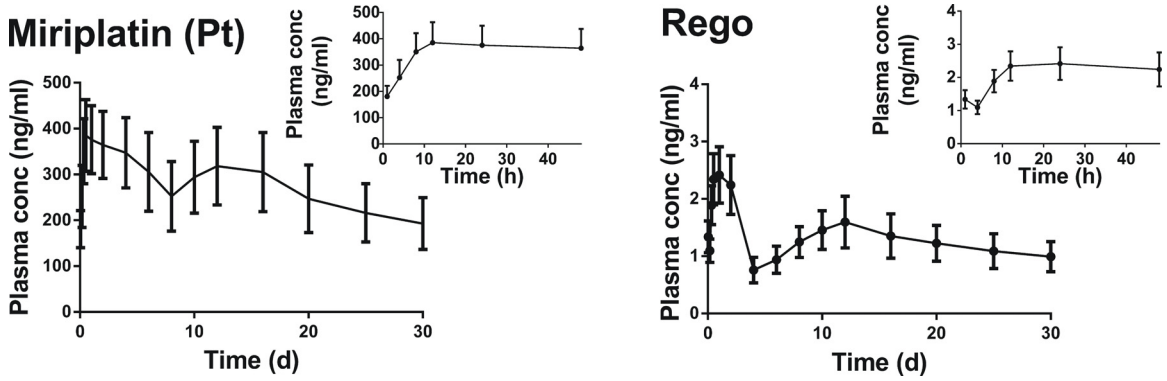

Fig. 8 – Plasma concentration profiles of miriplatin (Pt) and REGO after TACE in rabbits. Data are expressed as the means ± SD ($n = 6$).

monotherapy group ($P < 0.05$). On day 17, animals in blank microspheres group performed a high average tumor weight of 1.62 g (Fig. 9B). The animals treated with miriplatin alone, REGO microspheres, and in combination exhibited lower mean tumor weight of 0.70 g, 0.56 g and 0.48 g, respectively. A significantly lower mean tumor weight was obvious for miriplatin plus REGO microspheres compared to miriplatin alone ($P < 0.05$).

The results in Fig. 9 supported our design that the local sustained release of anti-angiogenic REGO from microspheres could potentiate the anticancer efficacy of chemotherapeutic miriplatin in HepG2 xenograft tumor model. There were promising therapeutic effects of locally delivering anti-angiogenic REGO with TACE for treatment of liver cancers. The improved therapeutic effects generated from REGO microspheres could result from the mechanism of action of REGO in treatment. As detection, the tumor cell proliferation was inhibited by REGO, similar to other chemotherapeutic drugs. This was suggested in Fig. 6 regarding *in vitro* cytotoxic effect of REGO released from microspheres on HepG2 cells. Moreover, REGO could also suppress multiple protein kinases, such as stromal and angiogenic kinases (VEGFR, TIE2, PDGFR-β and FGFR), tumorigenic kinases (KIT, RET, RAF-1, BRAF and mutant BRAF). These kinases could promote tumor neovascularization, vessel stabilization and lymphatic vessel formation and thus play an important role in tumor microenvironment, which was contributed to tumor deterioration and metastasis [13,43,44]. Therefore, REGO could suppress the angiogenesis by reducing associated protein kinases induced by TACE. Indeed, the anti-angiogenic effect of REGO mediated by microspheres have been demonstrated in Fig. 7. Moreover, the effects of REGO-mediated normalization of the tumor vasculature might elevate the efficacy of miriplatin monotherapy. Previous study demonstrated that REGO could normalize the tumor vasculature when combined with irinotecan in oxaliplatin-refractory patient-derived colorectal cancer xenografts, and the combination significantly delayed

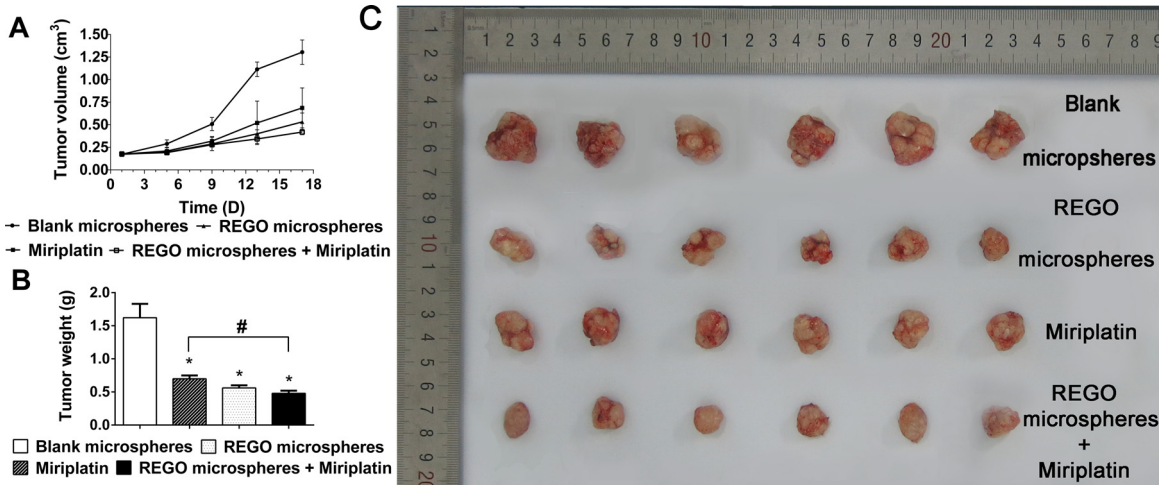

Fig. 9 – Antitumor activity of REGO microspheres and miriplatin alone or combination in BALB/c mice bearing HepG-2 cells. (A) Tumor growth curves for each group. (B) Tumor weight measured on day 17 after the experiment. (C) The images of excised tumors in mice collected after sacrifice. Data are expressed as the means ± SD ($n = 6$). $^{*}P < 0.05$, compared with control, $^{\#}P < 0.05$ compared with miriplatin alone.

tumor growth [45]. As mentioned in a previous report, anti-angiogenic agents with tumor normalizing potential have also documented antitumor activity against HCC [46]. Last but not least, REGO could reduce the drug resistance of HepG-2 induced by miriplatin, as demonstrated in our *in vitro* investigation (Fig. 5). Numerous studies have shown that REGO would antagonize drug resistance and provide an improved treatment efficacy combined with chemotherapy [40,42,47].

3.10. *Outlook*

The REGO-loaded PLGA microspheres provide more possibilities in adjusting drug loading, particle size and drug release. When altering PLGA type (molecular weight, the ration of lactic to glycolic acid), formulation composition, and preparation process, we could fine-tune the above characterizations for clinical application, which is especially meaningful for TACE treatment. As a result of the numerous factors for the therapeutic effect of TACE such as tumor burden, liver functions, and response to previous treatments, there was not any standardized protocol in TACE including chemotherapeutic drugs, dosage, injection rate, time interval between treatments and *etc.* [2,34]. In our study, PLGA microspheres was able to carry multiple chemotherapeutic drugs or drug combinations, with adjustable drug loading, particle size and drug release profiles, thus as a platform technology useful for TACE personalized therapy.

With the development of molecular targeted antiangiogenic therapy and recent advances in understanding HCC pathophysiology, the novel targeted combination strategies are emerging. The REGO microspheres prepared for TACE in this study have performed the promising benefits to improving the effects of TACE, and could be a novel therapy regiment for TACE. In addition to antiangiogenic effects, REGO shared a certain cytotoxic efficacy and mediated capacity of normalization of the tumor vasculature and potential to overcome drug resistance of chemotherapy, which was contributed to the increased therapeutic potency of TACE. Due to the complexity of HCC treatment including TACE balance between the therapeutic effect and unexpected stimulation of tumor angiogenesis, the optimal dose and regimen of REGO in combination with TACE needs to be extensively explored further.

In the present study, our preliminary *in vivo* results via adopting simpler administration in mice were promising to prove the concept of novel treatment strategy; however, it is worthy further *in vivo* study. In this regard, REGO microspheres will be administrated via TACE into animals bearing liver tumor. For example, rabbit VX2 liver tumor model which is a common animal model for evaluating therapeutic safety and effect in TACE [48–50], may be adopted in future studies including pharmacokinetics and antitumor effects, if resources allow.

4. Conclusions

In this study, PLGA microspheres has been introduced to incorporate an orally multikinase inhibitor REGO. The fabricated REGO microspheres provided sustained drug release for more than 30 d *in vitro* and *in vivo* after TACE. The microspheres demonstrated enhanced cytotoxic effects of miriplatin on HepG2 cells *in vitro*. More interestingly, an intense anti-angiogenic effect and the potential of antagonizing chemotherapeutic miriplatin resistance were observed *in vitro*. Moreover, *in vivo* investigation in a HepG2 xenograft tumor model demonstrated the outstanding antitumor efficacy of REGO microspheres significantly in superior to miriplatin monotherapy. In summary, the results of this study demonstrated that REGO microspheres for local delivery as a novel combination strategy with TACE may enhance the therapeutic potency of TACE for the treatment of HCC, and has promising clinical implications in future.

Conflicts of interest

The authors report no conflicts of interest in this work.

Acknowledgements

The authors gratefully acknowledge the National Natural Science Foundation of China (81872819 and 81573379), Natural Science Foundation of Jiangsu Province (BK20171390). This study was also supported by "Double First-Class" University project (CPU2018GY26), the Project of State Key Laboratory of Natural Medicines, China Pharmaceutical University (SKLNMZZCX201816) and the financial support from Development Funds for Priority Academic Programs in Jiangsu Higher Education Institutions. The authors finally thank Public platform of State Key Laboratory of Natural Medicines for assistance with scanning electron microscopy.

Supplementary materials

Supplementary material associated with this article can be found, in the online version, at doi:10.1016/j.ajps.2020.01.001.

REFERENCES

[1] Rahbari NN, Arianeb M, Mollberg NM, Müller SA, Moritz K, Büchler MW, et al. Hepatocellular carcinoma: current management and perspectives for the future. Ann Surg 2011;253(3):453.
[2] Lau WY, Yu SC, Lai EC, Leung TW. Transarterial chemoembolization for hepatocellular carcinoma. J Am Coll Surg 2006;202(1):155–68.
[3] Fuchs K, Duran R, Denys A, Bize PE, Borchard G, Jordan O. Drug-eluting embolic microspheres for local drug delivery–State of the art. J Control Release 2017;262:127–38.
[4] Poursaid A, Jensen MM, Huo E, Ghandehari H. Polymeric materials for embolic and chemoembolic applications. J Control Release 2016;240:414–33.
[5] Wang B, Xu H, Gao ZQ, Ning HF, Sun YQ, Cao GW. Increased expression of vascular endothelial growth factor in hepatocellular carcinoma after transcatheter arterial chemoembolization. Acta Radiol 2008;49(5):523–9.
[6] Ranieri G, Ammendola M, Marech I, Laterza A, Abbate I, Oakley C, et al. Vascular endothelial growth factor and tryptase changes after chemoembolization in hepatocarcinoma patients. World J Gastroenterol 2015;21(19):6018.
[7] Hyun SJ, Joong-Won P, Hoon KJ, Min A, Sun-Young K, Byung-Ho N, et al. Association between increment of serum VEGF level and prognosis after transcatheter arterial chemoembolization in hepatocellular carcinoma patients. Cancer Sci 2008;99(10):2037–44.
[8] Varghese J, Kedarisetty C, Venkataraman J, Srinivasan V, Deepashree T, Uthappa M, et al. Combination of TACE and sorafenib improves outcomes in BCLC stages B/C of hepatocellular carcinoma: a single centre experience. Ann Hepatol 2017;16(2):247–54.
[9] Pawlik TM, Reyes DK, David C, Kamel IR, Nikhil B, Geschwind JFH. Phase II trial of sorafenib combined with concurrent transarterial chemoembolization with drug-eluting beads for hepatocellular carcinoma. J Clin Oncol 2011;29(30):3960–7.
[10] Park JW, Koh YH, Kim HB, Kim HY, An S, Choi JI, et al. Phase II study of concurrent transarterial chemoembolization and sorafenib in patients with unresectable hepatocellular carcinoma. J Hepatol 2012;56(6):1336–42.
[11] Masatoshi K, Kazuho I, Nobuyuki C, Kohei N, Won-Young T, Tadatoshi T, et al. Phase III study of sorafenib after transarterial chemoembolisation in Japanese and Korean patients with unresectable hepatocellular carcinoma. Eur J Cancer 2011;47(14):2117–27.
[12] Lencioni R, Llovet JM, Han G, Tak WY, Yang J, Guglielmi A, et al. Sorafenib or placebo plus TACE with doxorubicin-eluting beads for intermediate stage HCC: the space trial. J Hepatol 2016;64(5):1090–8.
[13] Wilhelm SM, Jacques D, Lila A, Mark L, Carter CA, Gunnar S, et al. Regorafenib (BAY 73-4506): a new oral multikinase inhibitor of angiogenic, stromal and oncogenic receptor tyrosine kinases with potent preclinical antitumor activity. Int J Cancer 2011;129(1):245–55.
[14] Dirk S, Beate S. Regorafenib for cancer. Expert Opin Investig Drugs 2012;21(6):879–89.
[15] Demetri GD, Reichardt P, Kang YK, Blay JY, Rutkowski P, Gelderblom H, et al. Efficacy and safety of regorafenib for advanced gastrointestinal stromal tumours after failure of imatinib and sunitinib (GRID): an international, multicentre, randomised, placebo-controlled, phase 3 trial. Lancet 2013;381(9863):295–302.
[16] Grothey A, Cutsem EV, Sobrero A, Siena S, Falcone A, Ychou M, et al. Regorafenib monotherapy for previously treated metastatic colorectal cancer (CORRECT): an international, multicentre, randomised, placebo-controlled, phase 3 trial. Lancet 2013;381(9863):303–12.
[17] Rimassa L, Pressiani T, Personeni N, Santoro A. Regorafenib for the treatment of unresectable hepatocellular carcinoma. Expert Rev Anticancer Ther 2017;17(7):567–76.
[18] C Damiano G, Girolamo R. Trans-arterial chemoembolization as a therapy for liver tumours: new clinical developments and suggestions for combination with angiogenesis inhibitors. Crit Rev Oncol Hematol 2011;80(1):40–53.
[19] Ramazani F, Chen W, Nostrum CF, Van Storm G, Kiessling F, Lammers T, et al. Formulation and characterization of microspheres loaded with imatinib for sustained delivery. Int J Pharm 2015;482(1–2):123–30.
[20] Wang Y, Molin DG, Sevrin C, Grandfils C, Nm VDA, Gagliardi M, et al. *In vitro* and *in vivo* evaluation of drug-eluting microspheres designed for transarterial chemoembolization therapy. Int J Pharm 2016;503(1–2):150–62.
[21] Christian W, Schwendeman SP. Principles of encapsulating hydrophobic drugs in PLA/PLGA microparticles. Int J Pharm 2008;364(2):298–327.
[22] Jain RA. The manufacturing techniques of various drug loaded biodegradable poly(lactide-co-glycolide) (PLGA) devices. Biomaterials 2000;21(23):2475–90.
[23] Jin WC, Park JH, Song YB, Kim DD, Kim HC, Cho HJ. Doxorubicin-loaded poly(lactic-co-glycolic acid) microspheres prepared using the solid-in-oil-in-water method for the transarterial chemoembolization of a liver tumor. Colloids Surfaces B Biointerfaces 2015;132:305–12.
[24] Jeane C, Sheu AY, Weiguo L, Zhuoli Z, Dong-Hyun K, Lewandowski RJ, et al. Poly(lactide-co-glycolide) microspheres for MRI-monitored transcatheter delivery of sorafenib to liver tumors. J Control Release 2014;184(1):10–17.
[25] Yanai S, Okada H, Saito K, Kuge Y, Misaki M, Ogawa Y, et al. Optimal formulation of an angiogenesis inhibitor, TNP-470, for arterial injection determined by *in vitro* drug release and stability, and *in vivo* antitumor activity. Int J Pharm 1995;123(2):237–45.
[26] Hanada M, Baba A, Tsutsumishita Y, Noguchi T, Yamaoka T, Chiba N, et al. Intra-hepatic arterial administration with

miriplatin suspended in an oily lymphographic agent inhibits the growth of tumors implanted in rat livers by inducing platinum-DNA adducts to form and massive apoptosis. Cancer Chemother Pharmacol 2009;64(3):473–83.
[27] Takuji O, Hiroshi K, Hiroshi I, Masatoshi K, Michio S, Katsuaki T, et al. A randomized phase II trial of intra-arterial chemotherapy using SM-11355 (Miriplatin) for hepatocellular carcinoma. Invest New Drugs 2012;30(5):2015–25.
[28] Graves RA, Thomas F, Sarala P, Natalie P, Raisa M, Mandal TK. Effect of co-solvents on the characteristics of enkephalin microcapsules. J Biomater Sci Polym Ed 2006;17(6):709–20.
[29] Shenderova A, Burke TG, Schwendeman SP. Stabilization of 10-hydroxycamptothecin in poly(lactide-co-glycolide) microsphere delivery vehicles. Pharm Res 1997;14(10):1406–14.
[30] Jing WF, Hwa WC. Sustained release of etanidazole from spray dried microspheres prepared by non-halogenated solvents. J Control Release 2002;81(3):263–80.
[31] Itoabc F, Honnami H, Kawakami H, Kanamura K, Makino K. Study of types and mixture ratio of organic solvent used to dissolve polymers for preparation of drug-containing PLGA microspheres. Eur Polym J 2009;45(3):658–67.
[32] Rawat A, Burgess DJ. Effect of ethanol as a processing co-solvent on the PLGA microsphere characteristics. Int J Pharm 2010;394(1):99–105.
[33] Sah H. Microencapsulation techniques using ethyl acetate as a dispersed solvent: effects of its extraction rate on the characteristics of PLGA microspheres. J Control Release 1997;47(3):233–45.
[34] Giunchedi P, Maestri M, Gavini E, Dionigi P, Rassu G. Transarterial chemoembolization of hepatocellular carcinoma - agents and drugs:an overview. Part 2. Expert Opin Drug Deliv 2013;10(6):799–810.
[35] Wang J, Wang BM, Schwendeman SP. Characterization of the initial burst release of a model peptide from poly(d,l -lactide-co-glycolide) microspheres. J Control Release 2002;82(2):289–307.
[36] Hyun SJ, Joong-Won P, Hoon KJ, Min A, Sun-Young K, Byung-Ho N, et al. Association between increment of serum VEGF level and prognosis after transcatheter arterial chemoembolization in hepatocellular carcinoma patients. Cancer Sci 2010;99(10):2037–44.
[37] Li X, Feng GS, Zheng CS, Zhuo CK, Liu X. Expression of plasma vascular endothelial growth factor in patients with hepatocellular carcinoma and effect of transcatheter arterial chemoembolization therapy on plasma vascular endothelial growth factor level. World J Gastroenterol 2004;10(19):2878–82.
[38] Zhang H, Gao S. Temozolomide/PLGA microparticles and antitumor activity against glioma C6 cancer cells *in vitro*. Int J Pharm 2007;329(1–2):122–8.
[39] Fredenberg S, Wahlgren M, Reslow M, Axelsson A. The mechanisms of drug release in poly(lactic-co-glycolic acid)-based drug delivery systems-a review. Int J Pharm 2011;415(1–2):34–52.
[40] Wang YJ, Zhang YK, Zhang GN, Rihani SBA, Wei MN, Gupta P, et al. Regorafenib overcomes chemotherapeutic multidrug resistance mediated by ABCB1 transporter in colorectal cancer: *in vitro* and *in vivo* study. Cancer Lett 2017; 396:145–54.
[41] Marks EI, Tan C, Zhang J, Zhou L, Yang Z, Scicchitano A, et al. Regorafenib with a fluoropyrimidine for metastatic colorectal cancer after progression on multiple 5-FU-containing combination therapies and regorafenib monotherapy. Cancer Biol Ther 2015;16(12):1710–19.
[42] Zhang YK, Wang YJ, Lei ZN, Zhang GN, Zhang XY, Wang DS, et al. Regorafenib antagonizes BCRP-mediated multidrug resistance in colon cancer. Cancer Lett 2019; 442:104–12.
[43] Zopf D, Fichtner I, Bhargava A, Steinke W, Thierauch KH, Diefenbach K, et al. Pharmacologic activity and pharmacokinetics of metabolites of regorafenib in preclinical models. Cancer Med 2016;5(11):3176–85.
[44] Thillai K, Srikandarajah K, Ross P. Regorafenib as treatment for patients with advanced hepatocellular cancer. Future Oncol 2017;13(25):2223–32.
[45] Roberta S, Jens H, Michael B, Ajay B, Tina M, Nicole K, et al. Regorafenib (BAY 73-4506): antitumor and antimetastatic activities in preclinical models of colorectal cancer. Int J Cancer 2014;135(6):1487–96.
[46] Liu K, Zhang X, Xu W, Chen J, Yu J, Gamble JR, et al. Targeting the vasculature in hepatocellular carcinoma treatment: starving *versus* normalizing blood supply. Clin Transl Gastroenterol 2017;8(6):e98.
[47] Cai MH, Xu XG, Yan SL, Sun Z, Ying Y, Wang BK, et al. Regorafenib suppresses colon tumorigenesis and the generation of drug resistant cancer stem-like cells via modulation of miR-34a associated signaling. J Exp Clin Cancer Res 2018;37(1):151.
[48] Liang YJ, Yu H, Feng G, Zhuang L, Xi W, Ma M, et al. High-performance PLGA-magnetic microspheres prepared by rotating membrane emulsification for transcatheter arterial embolization and magnetic ablation in VX2 liver tumors. ACS Appl Mate Interfaces 2017;9(50):43478–89.
[49] Kim GM, Kim MD, Kim DY, Kim SH, Won JY, Park SI, et al. Transarterial chemoembolization using sorafenib in a rabbit VX2 liver tumor model: pharmacokinetics and antitumor effect. J Vasc Interv Radiol 2016;27(7):1086–92.
[50] Lee KH, Liapi E, Ventura VP, Buijs M, Vossen JA, Vali M, Geschwind JF. Evaluation of different calibrated spherical polyvinyl alcohol microspheres in transcatheter arterial chemoembolization: VX2 tumor model in rabbit liver. J Vasc Interv Radiol 2008;19(7):1065–9.
[51] Rowell RL. Physical chemistry of surfaces, 6th ed. J Colloid Interface Sci 1998;208(2):582.
[52] Smallwood IM. Handbook of organic solvent properties. Oxford: Butterworth-Heinemann; 2012.
[53] Sah H. Protein behavior at the water/methylene chloride interface. J Pharm Sci 2010;88(12):1320–5.